

Orientation of Nd^{3+} dipoles in yttrium aluminium garnet : a simple yet accurate model

Sylvain Schwartz^{1,*} and Gilles Feugnet¹, Maxence Rebut¹, Fabien Bretenaker², and Jean-Paul Pocholle¹

¹*Thales Research and Technology France, Campus Polytechnique,
1 avenue Augustin Fresnel, F-91767 Palaiseau Cedex, France*

²*Laboratoire Aimé Cotton, CNRS - Université Paris Sud 11, Campus d'Orsay, F-91405 Orsay Cedex, France*

(Dated: November 21, 2018)

We report an experimental study of the 1.064 μm transition dipoles in neodymium doped yttrium aluminium garnet (Nd-YAG) by measuring the coupling constant between two orthogonal modes of a laser cavity for different cuts of the YAG gain crystal. We propose a theoretical model in which the transition dipoles, slightly elliptic, are oriented along the crystallographic axes. Our experimental measurements show a very good quantitative agreement with this model, and predict a dipole ellipticity between 2% and 3%. This work provides an experimental evidence for the simple description in which transition dipoles and crystallographic axes are collinear in Nd-YAG (with an accuracy better than 1 deg), a point that has been discussed for years.

PACS numbers: 42.70.Hj, 42.55.Rz

While Nd-YAG is one of the most (if not the most) commonly used solid-state laser crystals, the exact orientation of transition dipoles within it is still, paradoxically, an unresolved problem. This is probably owing to the fact that for most applications it is sufficient to consider the Nd-YAG crystal (usually grown along the $\langle 111 \rangle$ crystallographic axis) as isotropic, although it has been known for long [1, 2] that Nd^{3+} ions in this configuration rather see a D_2 symmetry, with six possible dodecahedral orientations. The influence of crystal symmetry on dipole orientations has been previously studied in saturable absorbers such as Cr-YAG [3, 4, 5] and Tm-YAG [6, 7]. In the first case, it has been clearly established that transition dipoles were aligned with the crystal axes (labeled $\langle 100 \rangle$, $\langle 010 \rangle$ and $\langle 001 \rangle$) [4, 5] while in the second case it has been found that they were rather collinear with the $\langle 110 \rangle$, $\langle 011 \rangle$ and $\langle 101 \rangle$ directions [7]. In the case of Nd-YAG, the answer to this question is still unclear in spite of several previous studies involving in particular dynamical polarization effects in Nd-YAG lasers [8, 9, 10, 11].

In this paper, we propose a new approach to probe the orientation of transition dipoles in Nd-YAG, by measuring the coupling constant between two linearly-polarized orthogonal modes of a laser cavity for different cuts of the gain crystal, using a steady-state method similar to the one described in [12]. The measured coupling constant is a dimensionless ratio between cross-saturation and self-saturation coefficients, which is relatively independent of most laser parameters (pumping rate, birefringence, . . .), hence a good indicator for testing the validity of theoretical models. Our study deals for the most part with the 1064.15 nm emission line, sometimes referred to as R2, between the upper doublet of ${}^4F_{3/2}$ and the Y3 level of ${}^4I_{11/2}$. As a matter of fact, it is known from previous studies [13, 14] that the R1 line at 1064.4 nm (between the lower doublet of ${}^4F_{3/2}$ and the Y2 level of ${}^4I_{11/2}$) has a very small contribution to the overall gain, especially

at low pumping rates.

The paper is organized as follows. We first propose a theoretical model for calculating the coupling constant between two orthogonal modes of a Nd-YAG laser cavity, on the assumption that transition dipoles are collinear with YAG crystallographic axes. Starting from the very simple case of linear transition dipoles, we then generalize the model to the case of (slightly) elliptical dipoles, showing a very good agreement with the experimental value of the coupling constant published in [12] with $\langle 111 \rangle$ -cut Nd-YAG. We then apply this model to the description of our own experimental configuration, namely a two-mode laser cavity using as a gain medium a Nd-YAG crystal either $\langle 111 \rangle$ or $\langle 100 \rangle$ -cut. In both cases, the measured value of the coupling constant is compared with the corresponding theoretical prediction. The results, implications and perspectives of this work are finally discussed.

EXPRESSION OF THE COUPLING CONSTANT IN THE CASE OF LINEAR DIPOLES

In the usual semiclassical description of lasers, the transition dipole is often modeled by an operator $\hat{\mathbf{d}}$ associated with the linear vector $\mathbf{d} = d\mathbf{u}$, whose interaction with a linearly-polarized electric field $\mathbf{E} = E\mathbf{x}$ is described quantum mechanically by the dipolar Hamiltonian $-\hat{\mathbf{d}} \cdot \mathbf{E}$. Assuming furthermore that dipole coherence lifetime is much shorter than photon lifetime τ and population inversion lifetime T_1 (which is indeed the case in Nd-YAG lasers [15]), the dipolar interaction can be described by the following terms in the rate equations for the population inversion density N and field intensity I

[15] :

$$\begin{cases} \left. \frac{dN}{dt} \right|_{\text{int}} = -\frac{N}{T_1} \frac{I}{I_s} \cos^2(\widehat{\mathbf{x}}, \widehat{\mathbf{u}}) , \\ \left. \frac{dI}{dt} \right|_{\text{int}} = \sigma c N I \cos^2(\widehat{\mathbf{x}}, \widehat{\mathbf{u}}) , \end{cases} \quad (1)$$

where I_s is the saturation intensity, σ the interaction cross section, c the speed of light in vacuum, and where \mathbf{u} and \mathbf{x} are assumed to be unit vectors. The overall rate equations for I and N in a simple Lamb's laser model then read [15] :

$$\frac{dN}{dt} = W - \frac{N}{T_1} + \left. \frac{dN}{dt} \right|_{\text{int}} \quad \text{and} \quad \frac{dI}{dt} = -\frac{I}{\tau} + \left. \frac{dI}{dt} \right|_{\text{int}} , \quad (2)$$

where W is the pumping rate. As regards Nd-YAG lasers, the latter equations are sufficient to describe satisfactorily most of the experimentally observed phenomena such as relaxation oscillations [16] or spiking during laser turn-on [17]. However, they do not allow an accurate description of mode coupling in a Nd-YAG laser cavity [12].

General expression of the coupling constant

To this end, one must take into account, in addition with the two laser modes, the existence of several possible orientations for the transition dipoles. In the following model, we shall assume three possible orientations corresponding to the unitary vectors \mathbf{u}_1 , \mathbf{u}_2 and \mathbf{u}_3 , and associated with population inversion densities N_1 , N_2 and N_3 . We furthermore consider, in keeping with [12] and with the experiment described later on in this paper, the case of a laser with two modes linearly polarized along the \mathbf{x}_1 and \mathbf{x}_2 unitary vectors, and associated with intensities I_1 and I_2 . The semiclassical equations for the dipolar interaction (1) can be generalized as follows :

$$\begin{cases} \left. \frac{dN_i}{dt} \right|_{\text{int}} = -\frac{N_i}{T_1} \sum_{j=1,2} \frac{I_j}{I_s^j} \cos^2(\widehat{\mathbf{x}}_j, \widehat{\mathbf{u}}_i) , \\ \left. \frac{dI_j}{dt} \right|_{\text{int}} = \sigma c I_j \sum_{i=1}^3 N_i \cos^2(\widehat{\mathbf{x}}_j, \widehat{\mathbf{u}}_i) , \end{cases} \quad (3)$$

where we have introduced two possibly different saturation intensities I_s^1 and I_s^2 . The overall rate equations (2) for N_i and I_j become in this case :

$$\frac{dN_i}{dt} = W - \frac{N_i}{T_1} + \left. \frac{dN_i}{dt} \right|_{\text{int}} \quad \text{and} \quad \frac{dI_j}{dt} = -\frac{I_j}{\tau_j} + \left. \frac{dI_j}{dt} \right|_{\text{int}} , \quad (4)$$

where we have introduced different loss coefficients for each mode $\gamma_j = 1/\tau_j$. In equations (4), W has been chosen to be independent of i , which corresponds to the case of isotropic pumping (this has been checked experimentally, see further in this paper). In the steady-state

regime and for near-threshold operation (i.e. $I_j/I_s^j \ll 1$), equations (3) and (4) can be rewritten as :

$$N_i = W T_1 \left[1 - \sum_{j=1,2} \frac{I_j}{I_s^j} \cos^2(\widehat{\mathbf{x}}_j, \widehat{\mathbf{u}}_i) \right] , \quad (5)$$

and :

$$\gamma_j = \sigma c \sum_{i=1}^3 N_i \cos^2(\widehat{\mathbf{x}}_j, \widehat{\mathbf{u}}_i) . \quad (6)$$

The coupling constant C , initially defined by Lamb as the ratio between cross-saturation coefficients and self-saturation coefficients [18] in the case of lasers with short population inversion lifetime ($T_1 \ll \tau$), can be generalized to other kinds of lasers like Nd-YAG by the following (more general) definition, involving small variations from the steady-state regime [12] :

$$C = \frac{(\Delta I_1/\Delta \gamma_2)(\Delta I_2/\Delta \gamma_1)}{(\Delta I_1/\Delta \gamma_1)(\Delta I_2/\Delta \gamma_2)} . \quad (7)$$

Using this definition, a straightforward calculation starting from equations (6) and using equations (5) for the expression of N_i leads to the following formula :

$$C = \frac{\left(\sum_{i=1}^3 \cos^2(\widehat{\mathbf{x}}_1, \widehat{\mathbf{u}}_i) \cos^2(\widehat{\mathbf{x}}_2, \widehat{\mathbf{u}}_i) \right)^2}{\sum_{i=1}^3 \cos^4(\widehat{\mathbf{x}}_1, \widehat{\mathbf{u}}_i) \sum_{i=1}^3 \cos^4(\widehat{\mathbf{x}}_2, \widehat{\mathbf{u}}_i)} . \quad (8)$$

One important point is that this expression depends only on the overall geometry, making the coupling constant a useful tool for studying dipoles orientation.

Application to the case of the $\langle 111 \rangle$ crystal

The case of the $\langle 111 \rangle$ crystal is by far the most common for Nd-YAG lasers. In this configuration, the laser wave-vector \mathbf{k} is along the $\langle 111 \rangle$ axis, while the laser electric field lies in the transverse plane. Let us assume that the two laser modes are linearly polarized along the two following transverse unitary vectors :

$$\mathbf{x}_1 = \frac{1}{\sqrt{2}} \begin{pmatrix} 1 \\ -1 \\ 0 \end{pmatrix} \quad \text{and} \quad \mathbf{x}_2 = \frac{1}{\sqrt{6}} \begin{pmatrix} 1 \\ 1 \\ -2 \end{pmatrix} , \quad (9)$$

where the coordinates are expressed in the base of the crystallographic axes. Although this orthogonal base of the transverse plane has been arbitrarily chosen, it should be pointed out that this choice does not affect the final expression for the coupling constant (calculation shown in the appendix). Differently speaking, the coupling constant is independent, in the $\langle 111 \rangle$ case, of the crystal

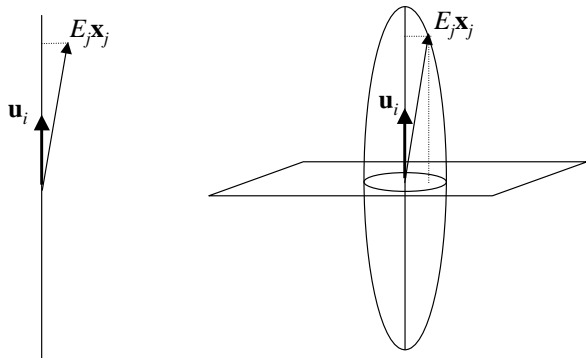


Figure 1: Comparison between usual linear dipole coupling (left) and elliptical dipole coupling (right). The latter has been phenomenologically introduced to allow for cross-coupling between dipoles from different sites.

orientation. Following the authors of [9], we consider transition dipoles $d\mathbf{u}_1$, $d\mathbf{u}_2$ and $d\mathbf{u}_3$ collinear with the crystal axes, namely :

$$\mathbf{u}_1 = \begin{pmatrix} 1 \\ 0 \\ 0 \end{pmatrix}, \quad \mathbf{u}_2 = \begin{pmatrix} 0 \\ 1 \\ 0 \end{pmatrix} \quad \text{and} \quad \mathbf{u}_3 = \begin{pmatrix} 0 \\ 0 \\ 1 \end{pmatrix}. \quad (10)$$

This hypothesis will be self-consistently confirmed by our experimental results later on in this paper. Expression (8) immediately leads in this case to the coupling constant value $C = 1/9 \simeq 0.11$.

This value can be compared with the experimental measurement $C \simeq 0.16 \pm 0.03$ from reference [12]. The discrepancy is attributed to the fact that dipoles from each site are not perfectly linear, but rather slightly elliptic, as will be described in what follows.

TAKING INTO ACCOUNT CROSS-COUPPLINGS BETWEEN DIPOLES FROM DIFFERENT CRYSTAL SITES

In order to account for possible cross-couplings between dipoles from different crystal sites, we shall assume a small dipole ellipticity $\beta \ll 1$. In this phenomenological description, illustrated on figure 1, the field-dipole interaction (3) takes the new following form :

$$\begin{cases} \left. \frac{dN_i}{dt} \right|_{\text{int}} = -\frac{N_i}{T_1} \sum_{j=1}^2 \frac{I_j}{I_s^j} [\cos^2(\widehat{\mathbf{x}_j, \mathbf{u}_i}) + \beta \sin^2(\widehat{\mathbf{x}_j, \mathbf{u}_i})], \\ \left. \frac{dI_j}{dt} \right|_{\text{int}} = \sigma c I_j \sum_{i=1}^3 N_i [\cos^2(\widehat{\mathbf{x}_j, \mathbf{u}_i}) + \beta \sin^2(\widehat{\mathbf{x}_j, \mathbf{u}_i})]. \end{cases}$$

This model will be used to calculate a new expression for the coupling constant in both the $\langle 111 \rangle$ and $\langle 100 \rangle$ cases.

Case of the $\langle 111 \rangle$ crystal

The latter equations can be applied to the previously-studied case of the $\langle 111 \rangle$ Nd-YAG crystal, using the vectors defined in (9) and (10). This leads to the following rate equations for the population inversion densities :

$$\begin{cases} \left. \frac{dN_1}{dt} \right|_{\text{int}} = -\frac{N_1}{T_1} \left[\frac{I_1}{I_s^1} \left(\frac{1}{2} + \frac{\beta}{2} \right) + \frac{I_2}{I_s^2} \left(\frac{1}{6} + \frac{5\beta}{6} \right) \right], \\ \left. \frac{dN_2}{dt} \right|_{\text{int}} = -\frac{N_2}{T_1} \left[\frac{I_1}{I_s^1} \left(\frac{1}{2} + \frac{\beta}{2} \right) + \frac{I_2}{I_s^2} \left(\frac{1}{6} + \frac{5\beta}{6} \right) \right], \\ \left. \frac{dN_3}{dt} \right|_{\text{int}} = -\frac{N_3}{T_1} \left[\frac{I_1}{I_s^1} \beta + \frac{I_2}{I_s^2} \left(\frac{2}{3} + \frac{\beta}{3} \right) \right], \end{cases}$$

and for the laser modes's intensities :

$$\begin{cases} \left. \frac{dI_1}{dt} \right|_{\text{int}} = \sigma c \left[\frac{N_1(1+\beta)}{2} + \frac{N_2(1+\beta)}{2} + N_3\beta \right] I_1, \\ \left. \frac{dI_2}{dt} \right|_{\text{int}} = \sigma c \left[\frac{(N_1 + N_2)(1+5\beta)}{6} + N_3 \frac{2+\beta}{3} \right] I_2. \end{cases}$$

We eventually obtain the following expression for the coupling constant in the presence of small elliptical dipolar coupling, up to the first order in β :

$$C = \frac{1}{9} + \frac{16}{9}\beta. \quad (11)$$

Based on the experimental result $C \simeq 0.16 \pm 0.03$ of reference [12], the estimate $\beta \simeq 2.75\% (\pm 0.5\%)$ can be deduced from expression (11). A possible explanation for this ellipticity is the existence of arbitrarily-oriented Nd^{3+} ions residing in defect sites of the YAG matrix, that would induce energy transfer between dipoles from different intrinsic crystal sites.

Case of the $\langle 100 \rangle$ crystal

We now turn to the case of a $\langle 100 \rangle$ crystal, on the reasonable assumption that dipole ellipticity β is independent of crystal cut. In this new configuration, the laser wave-vector \mathbf{k} is aligned with one crystallographic axis (say \mathbf{u}_3) and the two orthogonal laser modes are linearly polarized along two transverse axes defined by :

$$\mathbf{x}_1 = \begin{pmatrix} \cos \alpha \\ \sin \alpha \\ 0 \end{pmatrix} \quad \text{and} \quad \mathbf{x}_2 = \begin{pmatrix} -\sin \alpha \\ \cos \alpha \\ 0 \end{pmatrix},$$

where the coordinates have been expressed in the base $(\mathbf{u}_1, \mathbf{u}_2, \mathbf{u}_3)$ of the crystallographic axes. With the latter definition, the polarization directions of the two laser modes \mathbf{x}_1 and \mathbf{x}_2 make an angle α with the crystal (or dipoles) axes \mathbf{u}_1 and \mathbf{u}_2 . This leads, up to the first order

in β , to the following rate equations for the p inversion densities :

$$\begin{cases} \left. \frac{dN_1}{dt} \right|_{\text{int}} = -\frac{N_1}{T_1} \left[\frac{I_1}{I_s^1} A + \frac{I_2}{I_s^2} B \right], \\ \left. \frac{dN_2}{dt} \right|_{\text{int}} = -\frac{N_2}{T_1} \left[\frac{I_1}{I_s^1} B + \frac{I_2}{I_s^2} A \right], \end{cases}$$

where the following notations have been introduced

$$A = \cos^2 \alpha + \beta \sin^2 \alpha \quad \text{and} \quad B = \sin^2 \alpha + \beta \cos^2 \alpha$$

Similarly, one gets the following rate equations for the laser modes's intensities :

$$\begin{cases} \left. \frac{dI_1}{dt} \right|_{\text{int}} = \sigma c [N_1 A + N_2 B] I_1, \\ \left. \frac{dI_2}{dt} \right|_{\text{int}} = \sigma c [N_1 B + N_2 A] I_2. \end{cases}$$

It should be mentioned that the influence of the pump intensity has been neglected in this analysis since it would introduce corrections in terms on the order of β^2 or smaller. One final result is $C = 4A^2 B^2 / (A^2 + B^2)^2$, which reduces, up to first order in α^2 and β , to the following expression

$$C = 4(\alpha^2 + \beta)^2.$$

This expression will be used later on in this paper to compare this theoretical model with data from the experiment.

EXPERIMENT

We now turn to the description of our experimental setup, sketched in figure 2. We use a 18-cm-long laser cavity with a 2.5-cm-long Nd-YAG crystal gain medium. The cavity also contains a 10-cm-long uniaxial birefringent crystal (YVO₄) cut at 45° to its optical axis, in order to spatially separate the two orthogonal modes of the cavity. We have checked that the two perpendicular ordinary and extraordinary polarizations correspond to the two spatially separated modes inside the cavity and that no significant cross-coupling inducing forked eigenstate operation [19] was induced inside the Nd-YAG crystal (which imposes a specific crystal orientation in the $\langle 100 \rangle$ case, see further). We have also checked, using a Fabry-Perot analyzer, that each one of the two perpendicular laser modes was longitudinally single-mode. This is probably due to the fact that the YVO₄ crystal acts as an etalon and also due to the near-threshold operation of the laser.

The razor blades, placed in the vicinity of the two separated beams, are intended for creating additional

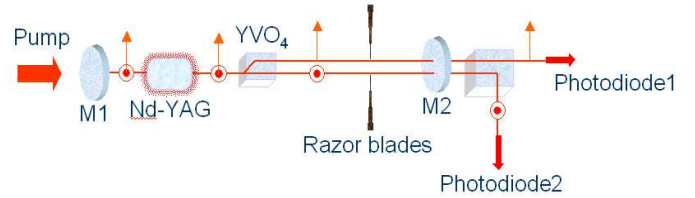


Figure 2: Sketch of our experimental laser cavity setup. Each razor blade can be translationally moved perpendicularly to the laser axis, in order to create additional losses to the corresponding laser mode. M1 and M2 are the cavity mirrors.

losses to the corresponding laser modes (i.e. changing γ_1 and γ_2). We limit the losses introduced by the razor blade to about 1%, allowing us to neglect the beam truncation and to keep a good overlap of the beams in the active medium. The intensities of the two orthogonal modes are then monitored on two photodiodes after being separated by a polarizing beam splitter. Typically, the position of one razor blade is changed periodically in time (using a piezoelectric transducer), and the relative dependence of I_1 and I_2 is monitored on an oscilloscope. We successively introduce razor blade losses to the 1 and 2 modes, thus obtaining experimental values for $(\Delta I_2 / \Delta \gamma_1) / (\Delta I_1 / \Delta \gamma_1)$ and $(\Delta I_1 / \Delta \gamma_2) / (\Delta I_2 / \Delta \gamma_2)$. The coupling constant is eventually deduced from expression (7).

It is worth noticing that this result is independent, at least in the framework of our theoretical model, of most laser parameters, in particular saturation intensities I_s^1 and I_s^2 , pumping rate and calibration of photodiodes. The dominant error source in this measurement is intensity self-modulation, which introduces an uncertainty in the slope measurement. Another error source is residual pumping anisotropy. In order to assess the contribution of the latter effect, we have checked experimentally that pumping light had no preferential polarization axis with an accuracy better than a few percents, resulting in a relative error of a few percents on the measurement of C . The overall measurement error is estimated to $\delta C / C \simeq 10\%$.

Case of the $\langle 111 \rangle$ Nd-YAG

In a first experiment, we use a typical $\langle 111 \rangle$ Nd-YAG crystal as a gain medium, with arbitrary orientation. The raw output light from the fibered laser diode is focused on the crystal for optical pumping. Following the method described above for the measurement of the coupling constant, we have obtained the data reported on figure 3. This leads to the following value : $C \simeq 0.15 \pm 0.015$, in very good agreement with the previously-published value $C \simeq 0.16 \pm 0.03$ [12]. This agreement is probably owing to

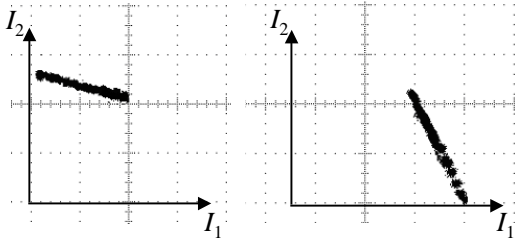


Figure 3: Experimental curves showing I_2 versus I_1 in the $\langle 111 \rangle$ case when the loss rates γ_1 (left curve) and γ_2 (right curve) are changed. Slopes measurements provide the following values : $(\Delta I_2/\Delta\gamma_1)/(\Delta I_1/\Delta\gamma_1) = -0.3 \pm 0.03$ (left curve) and $(\Delta I_1/\Delta\gamma_2)/(\Delta I_2/\Delta\gamma_2) = -0.5 \pm 0.05$, leading to $C = 0.15 \pm 0.015$.

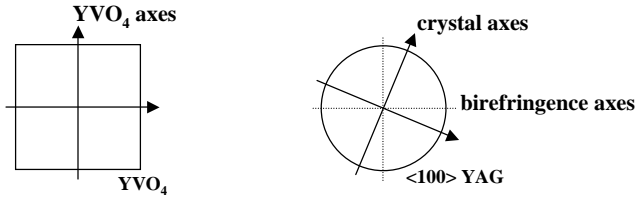


Figure 4: Relative orientation, around the longitudinal cavity axis, of the YVO_4 crystal (left) and the $\langle 100 \rangle$ Nd-YAG crystal (right). As can be seen on this sketch, the YAG crystal has been oriented in order to align its residual birefringence axes with the YVO_4 crystal axes, in order to ensure that the cavity eigenmodes are linearly polarized along the YVO_4 axes (instead of being forked modes).

the fact that the coupling constant is relatively independent of most laser parameters, as pointed out previously, provided the two cavity modes are properly separated by the YVO_4 crystal and spatial hole burning can be neglected (which can be shown to be the case here and in the work of reference [12]). Taking into account this new experimental value (with smaller error bars than in [12]), the following finer estimate of the ellipticity β can be deduced from equation (11) : $\beta \simeq 2.2\% (\pm 0.2\%)$.

Case of the $\langle 100 \rangle$ crystal

In a second experiment, the $\langle 111 \rangle$ gain medium is replaced by a $\langle 100 \rangle$ Nd-YAG crystal, manufactured by the German company FEE GmbH. The crystallographic axes are known precisely by X-ray analysis. A small birefringence is observed for this crystal, probably due to mechanical stress from the mount. In order to avoid the appearance of forked modes in the laser cavity [19], it is necessary to properly align the birefringence axis of the YAG crystal with the ordinary and extraordinary polarization axis of the YVO_4 crystal. As illustrated on figure 4, such a configuration is experimentally

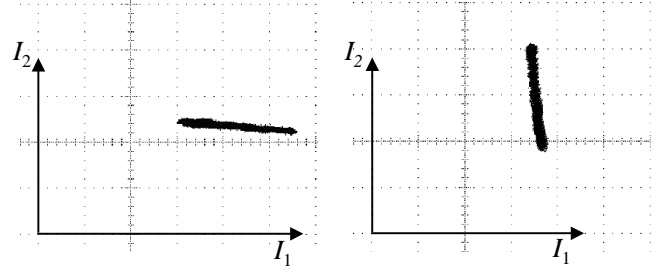


Figure 5: Experimental curves showing I_2 versus I_1 in the $\langle 100 \rangle$ case (angle between laser and crystal axes : 10 ± 1 deg) when the loss rates γ_1 (left curve) and γ_2 (right curve) are changed. Slopes measurements provide the following values : $(\Delta I_2/\Delta\gamma_1)/(\Delta I_1/\Delta\gamma_1) = -0.11 \pm 0.01$ (left curve) and $(\Delta I_1/\Delta\gamma_2)/(\Delta I_2/\Delta\gamma_2) = -0.1 \pm 0.01$, leading to $C = 0.011 \pm 0.001$.

obtained, on our setup, with an angle $\alpha = 10 \pm 1$ deg between the crystal axes and the YVO_4 axes. With such an alignment, the cavity eigenmodes are linearly polarized and coincide with the ordinary and extraordinary polarization axis of the YVO_4 crystal, making the experiment suitable for comparison with our theoretical model. It is then possible to measure the coupling constant between both orthogonal modes following the previously-described method, as reported on figure 5. The result is $C \simeq 0.011 \pm 0.001$, to be compared with the theoretical value predicted by our model (equation (13) with $\alpha = 10 \pm 1$ deg and $\beta \simeq 2.2\% \pm 0.2\%$), namely $C \simeq 0.011 \pm 0.001$. This remarkable agreement is an experimental evidence for the simple theoretical description proposed in this paper.

CONCLUSION

To summarize, we have proposed a simple yet accurate theoretical model for describing the orientation of transition dipoles in a Nd-YAG crystal, by making the following hypotheses : first, dipoles are slightly elliptic; second, their main directions are collinear with the crystallographic axes. This model has been tested by making experimental measurements of the coupling constant between two orthogonal modes of a Nd-YAG laser for two different crystal cuts ($\langle 111 \rangle$ and $\langle 100 \rangle$). A remarkable quantitative agreement between theory and experiment has been observed. In particular, this study is an experimental evidence for the fact that transition dipoles are indeed aligned with crystallographic axes of the Nd-YAG crystal, with an accuracy better than 1 deg.

The significant reduction of coupling between orthogonally polarized modes in a laser cavity using a $\langle 100 \rangle$ -cut gain medium, as demonstrated in this paper, could be

used to significantly increase the stability of bi-frequency lasers, with possible applications in the field of lidar or multioscillator ring laser gyroscopes. Our work predicts that the more favorable situation for such applications will occur when the crystallographic axes are aligned with the laser cavity axes, with a minimum achievable coupling constant as small as $4\beta^2 \simeq 2.5 \cdot 10^{-3}$. Furthermore, the simple and original protocol proposed in this paper could be applied to other kinds of solid-state gain media or saturable absorbers, in order to probe the orientation of their active dipoles.

The authors are happy to thank Philippe Goldner from Chimie ParisTech and Daniel Rytz from FEE GmbH for helpful discussions.

APPENDIX: CALCULATION OF THE COUPLING CONSTANT FOR AN ARBITRARY CRYSTAL ORIENTATION IN THE $\langle 111 \rangle$ CASE WITHOUT DIPOLE ELLIPTICITY

In this appendix, we will show that in the case of a $\langle 111 \rangle$ crystal with linear dipoles oriented along the crystallographic axes, the coupling constant is independent of the orientation between the crystal axes and the directions of the laser modes. To this end, we consider linear dipoles oriented along the crystallographic axes, namely :

$$\mathbf{u}_1 = \begin{pmatrix} 1 \\ 0 \\ 0 \end{pmatrix}, \quad \mathbf{u}_2 = \begin{pmatrix} 0 \\ 1 \\ 0 \end{pmatrix} \quad \text{and} \quad \mathbf{u}_3 = \begin{pmatrix} 0 \\ 0 \\ 1 \end{pmatrix}. \quad (14)$$

Any pair of orthogonal directions for the laser modes in the transverse plane can be obtained by rotating (by the appropriate angle α) the initial base defined by (9), which reads :

$$\begin{cases} \mathbf{x}_1 = \frac{\cos \alpha}{\sqrt{2}} \begin{pmatrix} 1 \\ -1 \\ 0 \end{pmatrix} + \frac{\sin \alpha}{\sqrt{6}} \begin{pmatrix} 1 \\ 1 \\ -2 \end{pmatrix}, \\ \mathbf{x}_2 = \frac{-\sin \alpha}{\sqrt{2}} \begin{pmatrix} 1 \\ -1 \\ 0 \end{pmatrix} + \frac{\cos \alpha}{\sqrt{6}} \begin{pmatrix} 1 \\ 1 \\ -2 \end{pmatrix}. \end{cases} \quad (15)$$

A straightforward although tedious calculation leads, from equations (14) and (15), to the following expression :

$$\sum_{i=1}^3 \cos^2(\widehat{\mathbf{x}_1, \mathbf{u}_i}) \cos^2(\widehat{\mathbf{x}_2, \mathbf{u}_i}) = \frac{1}{6}. \quad (16)$$

Similarly, we obtain :

$$\sum_{i=1}^3 \cos^4(\widehat{\mathbf{x}_1, \mathbf{u}_i}) = \frac{1}{2} \quad \text{and} \quad \sum_{i=1}^3 \cos^4(\widehat{\mathbf{x}_2, \mathbf{u}_i}) = \frac{1}{2}. \quad (17)$$

It is a remarkable fact that expressions (16) and (17) are independent of α . Using expression (8) for the coupling constant eventually leads to $C = 1/9$, independently of the orientation between the $\langle 111 \rangle$ crystal and the laser modes.

* Electronic address: sylvain.schwartz@thalesgroup.com

- [1] J. F. Dillon and L. R. Walker, Phys. Rev. **124**, 1401 (1961).
- [2] J. P. van der Ziel, M. D. Sturge and L. G. Van Uitert, Phys. Rev. Lett. **27** (8) 508 (1971).
- [3] H. Eilers, K. R. Hoffman, W. M. Dennis, S. M. Jacobsen and W. M. Yen, Appl. Phys. Lett. **61** (25) 2958 (1992).
- [4] A. Brignon, J. Opt. Soc. Am. B **13** (10) 2154 (1996).
- [5] M. Brunel, O. Emile, M. Vallet, F. Bretenaker, A. Le Floch, L. Fulbert, J. Marty, B. Ferrand and E. Molva, Phys. Rev. A **60** (5) 4052 (1999).
- [6] C. Greiner, B. Boggs, T. Loftus, T. Wang and T. W. Mossberg, Phys. Rev. A **60** (4) R2657 (1999).
- [7] Y. Sun, G. M. Wang, R. L. Cone, R. W. Equall and M. J. M. Leask, Phys. Rev. B **62** (23) 15443 (2000).
- [8] P. Esherick and A. Owyong, Proc. SPIE Vol. 912 2 (1988).
- [9] M. Lukač, S. Trošt and M. Kažič, IEEE Journal of Quantum Electronics **28** (11) 2560 (1992).
- [10] N. V. Kravtsov, E. G. Lariontsev and N. I. Naumkin, Quantum Electronics **34** (9) 839 (2004).
- [11] A. McKay, J. M. Dawes and J.-D. Park, Optics Express **15** (25) 16342 (2007).
- [12] M. Brunel, M. Vallet, A. Le Floch and F. Bretenaker, Appl. Phys. Lett. **70** (16) 2070 (1997).
- [13] Takashi Kushida, H. M. Marcos, and J. E. Geusic, Phys. Rev. **167**, 289 (1968).
- [14] K. Fuhrmann, N. Hodgson, F. Hollinger, and H. Weber, J. Appl. Phys. **62**, 4041 (1987).
- [15] A. Siegman, *Lasers*, University Science Books (1986).
- [16] C. Tang, J. Appl. Phys. **34**, 2935 (1963).
- [17] M. Lefebvre, D. Dangoisse and P. Glorieux, Phys. Rev. A **29**, 758 (1984).
- [18] M. Sargent III, M. O. Scully and W. E. Lamb Jr., *Laser Physics* (Addison-Wesley, Reading, MA, 1974).
- [19] F. Bretenaker and A. Le Floch, J. Opt. Soc. Am. B **8**, 230 (1991) and J. Opt. Soc. Am. B. **9**, 2295 (1992).